

Ergodic Rate Analysis of Reconfigurable Intelligent Surface-Aided Massive MIMO Systems with ZF Detectors

Kangda Zhi, Cunhua Pan, Hong Ren and Kezhi Wang

Abstract—This letter investigates the reconfigurable intelligent surface (RIS)-aided massive multiple-input multiple-output (MIMO) systems with a two-timescale design. First, the zero-forcing (ZF) detector is applied at the base station (BS) based on instantaneous aggregated CSI, which is the superposition of the direct channel and the cascaded user-RIS-BS channel. Then, by leveraging the channel statistical property, we derive the closed-form ergodic achievable rate expression. Using a gradient ascent method, we design the RIS passive beamforming only relying on the long-term statistical CSI. We prove that the ergodic rate can reap the gains on the order of $\mathcal{O}(\log_2(MN))$, where M and N denote the number of BS antennas and RIS elements, respectively. We also prove the striking superiority of the considered RIS-aided system with ZF detectors over the RIS-free systems and RIS-aided systems with maximum-ratio combining (MRC).

Index Terms—Reconfigurable intelligent surface (RIS), intelligent reflecting surface (IRS), statistical CSI, massive MIMO, ZF.

I. INTRODUCTION

As an emerging technique, reconfigurable intelligent surface (RIS) has been widely investigated and recognized as a cost-effective complement for future systems [1], [2]. Compared with the base stations (BSs) comprised of expensive radio-frequency chains, an appealing feature for the RIS is that it mainly contains low-cost and low energy consumption reflection elements. Therefore, integrating the RIS with a large number of elements into conventional systems can assist in creating high-quality transmission paths and efficiently improve the systems capacity [3], [4].

A well-acknowledged challenge for the RIS is that it may introduce heavy channel estimation overhead. Fortunately, a novel and more practical countermeasure, named as two-timescale beamforming design, has been proposed and validated by some contributions [5]–[9]. On one hand, the two-timescale scheme aims to design the passive RIS beamforming based on purely statistical channel state information (CSI), and this could effectively reduce the overhead and the energy consumption in the operation of the RIS. On the other hand, the two-timescale scheme designs the BS beamforming based

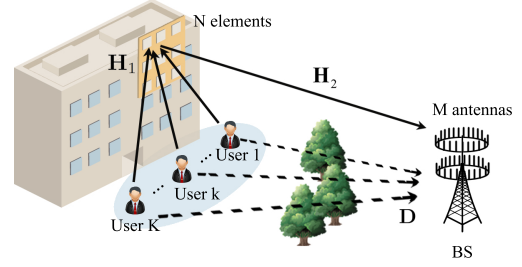


Fig. 1. Uplink transmission in RIS-aided massive MIMO systems.

on the instantaneous aggregated channel, which is the superposition of the direct channel and cascaded user-RIS-BS channel. As a result, the aggregated channel has the same dimension as that in conventional systems. Thus, two-timescale schemes possess the same channel estimation overhead as conventional systems.

Inspired by the above benefits, the two-timescale design has been recently exploited in RIS-aided massive MIMO systems [10]. It has demonstrated that by integrating an RIS into conventional massive MIMO systems, the rate performance can be significantly improved, especially when the original direct links are weak due to the blockage. However, only the simple maximum-ratio combining (MRC) detector was considered in [10], and it revealed that the achieved gains are limited by the multi-user interference. Therefore, it is expected that the zero-forcing (ZF) detector, which can effectively mitigate the interference, is more suitable for RIS-aided massive MIMO systems.

Against the above background, in this letter, we consider the RIS-aided massive MIMO systems with ZF detectors. We derive the closed-form expression for the ergodic rate, which only relies on the long-term CSI. We then design the RIS based on a gradient ascent algorithm. By analyzing the rate expression, we find that it can achieve a gain of order $\mathcal{O}(\log_2(MN))$, which validates the effectiveness of applying ZF detectors in RIS-aided massive MIMO systems.

II. SYSTEM MODEL

As illustrated in Fig. 1, the uplink transmission of a massive MIMO system is considered. Different from conventional systems, an RIS is introduced and deployed in the vicinity of the K single-antenna users to enhance the quality of service. The considered model is especially suitable for the scenario where some cell-edge users suffer service degradation. Denote the number of BS antennas and RIS elements as M and N ,

(Corresponding author: Cunhua Pan).

K. Zhi, C. Pan are with the School of Electronic Engineering and Computer Science at Queen Mary University of London, London E1 4NS, U.K. (e-mail: k.zhi, c.pan@qmul.ac.uk).

H. Ren is with the National Mobile Communications Research Laboratory, Southeast University, Nanjing 210096, China. (hren@seu.edu.cn).

K. Wang is with Department of Computer and Information Sciences, Northumbria University, UK. (e-mail: kezhi.wang@northumbria.ac.uk).

respectively, where $M > K$. Then, we can define the channel between the users and the RIS, the channel between the RIS and the BS, the direct channel between the users and the BS as $\mathbf{H}_1 \in \mathbb{C}^{N \times K}$, $\mathbf{H}_2 \in \mathbb{C}^{M \times N}$ and $\mathbf{D} \in \mathbb{C}^{M \times K}$, respectively.

Define the phase shift matrix of the RIS as $\Phi = \text{diag}\{\mathbf{v}^H\}$, where $\mathbf{v} = [e^{j\theta_1}, \dots, e^{j\theta_N}]^H$, and θ_n is the phase shift of the n -th RIS element. Herein, we can express the cascaded user-RIS-BS channel as $\mathbf{G} = \mathbf{H}_2\Phi\mathbf{H}_1 \in \mathbb{C}^{M \times K}$, and then express the aggregated channel from users to the BS as $\mathbf{Q} = \mathbf{G} + \mathbf{D} \in \mathbb{C}^{M \times K}$. It is worth noting that this aggregated channel \mathbf{Q} possesses the same dimension as conventional massive MIMO systems.

Based on the above definitions, we next present the detailed channel model for \mathbf{Q} . Firstly, considering that the direct links may be easily blocked [5], we adopt the Rayleigh channel model for \mathbf{D} as follows

$$\mathbf{D} = \tilde{\mathbf{D}}\Omega_d^{1/2}, \quad (1)$$

where $\Omega_d = \text{diag}\{\gamma_1, \dots, \gamma_K\}$, and γ_k denotes the distance-dependent path-loss factor. Each element of matrix $\tilde{\mathbf{D}} \in \mathbb{C}^{M \times K}$ is independent and identically distributed (i.i.d.) complex Gaussian random variables, whose mean is zero and variance is unit.

Next, since we consider that the RIS is deployed close to the users, and according to the fact that the RIS is often installed above the ground, we assume that the user-RIS channels have purely line-of-sight (LoS) paths. Then, we denote

$$\mathbf{H}_1 = [\sqrt{\alpha_1}\bar{\mathbf{h}}_1, \dots, \sqrt{\alpha_K}\bar{\mathbf{h}}_K], \quad (2)$$

where $\sqrt{\alpha_k}$ denotes the path loss. To specify the LoS channel $\bar{\mathbf{h}}_k$, we utilize the two-dimensional uniform squared planar array (USPA) model. The array response vector in USPA model can be expressed as follows

$$\mathbf{a}_X(\vartheta^a, \vartheta^e) = \begin{bmatrix} 1, \dots, e^{j2\pi \frac{d}{\lambda} (x \sin \vartheta^e \sin \vartheta^a + y \cos \vartheta^e)}, \\ \dots, e^{j2\pi \frac{d}{\lambda} ((\sqrt{X}-1) \sin \vartheta^e \sin \vartheta^a + (\sqrt{X}-1) \cos \vartheta^e)} \end{bmatrix}^T, \quad (3)$$

where ϑ^a and ϑ^e are azimuth and elevation angles in the propagation path, respectively. Therefore, we can now express $\bar{\mathbf{h}}_k = \mathbf{a}_N(\varphi_{kr}^a, \varphi_{kr}^e)$.

Since the RIS is placed near the users, the distance between the RIS and the BS could be a bit large. Even though both the RIS and the BS have certain heights, it is still not guaranteed that the RIS-BS channel is purely LoS. As a result, the Rician model is suitable for the considered RIS-BS channel. Besides, by adjusting the value of Rician factors, we can study the impacts of scatterers in RIS-aided systems. This feature is important, since many works have proven that rich scattering environment is beneficial in conventional massive MIMO systems [11], while the corresponding impact in RIS-aided massive MIMO systems with ZF detector is still unknown. Thus, we define

$$\mathbf{H}_2 = \sqrt{\frac{\beta\delta}{\delta+1}}\bar{\mathbf{H}}_2 + \sqrt{\frac{\beta}{\delta+1}}\tilde{\mathbf{H}}_2, \quad (4)$$

where β is path loss, δ represents the Rician factor. Note that the Rician factor, varying from 0 to ∞ , characterizes

the strength ratio between LoS and non-LoS (NLoS) paths. The NLoS path $\tilde{\mathbf{H}}_2$ contains i.i.d. complex Gaussian random variables with zero mean and unit variance. Recalling USPA model (3), the LoS path, $\bar{\mathbf{H}}_2$, is written as

$$\bar{\mathbf{H}}_2 = \mathbf{a}_M(\phi_r^a, \phi_r^e) \mathbf{a}_N^H(\varphi_t^a, \varphi_t^e) \triangleq \mathbf{a}_M \mathbf{a}_N^H, \quad (5)$$

where a notational simplification $\bar{\mathbf{H}}_2 \triangleq \mathbf{a}_M \mathbf{a}_N^H$ is applied in the sequel of this paper. Note that the rank of matrix $\bar{\mathbf{H}}_2$ is one. This means that when $\delta \rightarrow \infty$, the cascaded channel \mathbf{G} may become rank-deficient, and then the achievable spatial multiplexing gains may degrade.

We can now express the $M \times 1$ received signal vector at the BS as

$$\mathbf{y} = \sqrt{p}\mathbf{Q}\mathbf{x} + \mathbf{n} = \sqrt{p}(\mathbf{H}_2\Phi\mathbf{H}_1 + \mathbf{D})\mathbf{x} + \mathbf{n}, \quad (6)$$

where p denotes the average transmit power for each user, $\mathbf{x} = [x_1, \dots, x_K]^T$ denotes the transmit symbols from K users, and $\mathbf{n} \sim \mathcal{CN}(\mathbf{0}, \sigma^2 \mathbf{I}_M)$ is the noise vector.

We adopt the traditional channel estimation method in massive MIMO systems, where the $M \times K$ instantaneous CSI \mathbf{Q} is estimated perfectly in each small-scale channel coherence time. Therefore, in each channel coherence time, the ZF detector at the BS is set as

$$\mathbf{A} = \mathbf{Q}(\mathbf{Q}^H\mathbf{Q})^{-1}, \quad (7)$$

which results in $\mathbf{A}^H\mathbf{Q} = \mathbf{I}_K$.

Thus, the detected symbol vector is given by

$$\mathbf{r} = \mathbf{A}^H\mathbf{y} = \sqrt{p}\mathbf{x} + (\mathbf{Q}^H\mathbf{Q})^{-1}\mathbf{Q}^H\mathbf{n}. \quad (8)$$

Based on Jensen's inequality, a lower bound for the k -th user's ergodic achievable rate is given by

$$\begin{aligned} R_k &= \mathbb{E} \left\{ \log_2 \left(1 + \frac{p}{\left[(\mathbf{Q}^H\mathbf{Q})^{-1} \mathbf{Q}^H \mathbf{n} \left((\mathbf{Q}^H\mathbf{Q})^{-1} \mathbf{Q}^H \mathbf{n} \right)^H \right]_{kk}} \right) \right\} \\ &= \mathbb{E} \left\{ \log_2 \left(1 + \frac{p}{\sigma^2 \left[(\mathbf{Q}^H\mathbf{Q})^{-1} \right]_{kk}} \right) \right\} \\ &\geq \log_2 \left(1 + \frac{p}{\sigma^2 \mathbb{E} \left\{ \left[(\mathbf{Q}^H\mathbf{Q})^{-1} \right]_{kk} \right\}} \right). \end{aligned} \quad (9)$$

III. RATE ANALYSIS AND RIS DESIGN

In this section, we first derive the closed-form expression for the rate R_k , and then use the derived expression to propose a statistical CSI-based RIS design.

To derive R_k , we need to compute $\mathbb{E} \left\{ \left[(\mathbf{Q}^H\mathbf{Q})^{-1} \right]_{kk} \right\}$. To this end, we expand matrix \mathbf{Q}^H as

$$\mathbf{Q}^H = \sqrt{\frac{\beta\delta}{\delta+1}}\mathbf{H}_1^H\Phi\bar{\mathbf{H}}_2^H + \sqrt{\frac{\beta}{\delta+1}}\mathbf{H}_1^H\Phi\tilde{\mathbf{H}}_2^H + \Omega_d^{1/2}\tilde{\mathbf{D}}^H. \quad (10)$$

For ease of exposition, we define $\mathbf{Q}^H \triangleq [\mathbf{q}_1, \dots, \mathbf{q}_M]$, $\bar{\mathbf{H}}_2^H \triangleq [\bar{\mathbf{c}}_1, \dots, \bar{\mathbf{c}}_M]$, $\tilde{\mathbf{H}}_2^H \triangleq [\tilde{\mathbf{c}}_1, \dots, \tilde{\mathbf{c}}_M]$, and $\tilde{\mathbf{D}}^H \triangleq [\tilde{\mathbf{d}}_1, \dots, \tilde{\mathbf{d}}_M]$. Recalling that $\tilde{\mathbf{H}}_2$ and $\tilde{\mathbf{D}}$ are all comprised of

i.i.d. complex Gaussian variables, and $\tilde{\mathbf{H}}_2$ and $\tilde{\mathbf{D}}$ are mutual independent, we therefore have

$$\tilde{\mathbf{c}}_m \sim \mathcal{CN}(\mathbf{0}, \mathbf{I}_N), 1 \leq m \leq M, \quad (11)$$

$$\tilde{\mathbf{d}}_m \sim \mathcal{CN}(\mathbf{0}, \mathbf{I}_K), 1 \leq m \leq M, \quad (12)$$

where $\tilde{\mathbf{c}}_i$ and $\tilde{\mathbf{c}}_j$ are mutual independent for $i \neq j$; $\tilde{\mathbf{d}}_i$ and $\tilde{\mathbf{d}}_j$ are mutual independent, for $i \neq j$; $\tilde{\mathbf{c}}_i$ and $\tilde{\mathbf{d}}_j$ are mutual independent for all i and j . Then, since the linear transformation for a standard Gaussian random vector is still a Gaussian random vector [12], we obtain

$$\begin{aligned} & \sqrt{\frac{\beta\delta}{\delta+1}} \mathbf{H}_1^H \Phi^H \tilde{\mathbf{c}}_m + \sqrt{\frac{\beta}{\delta+1}} \mathbf{H}_1^H \Phi^H \tilde{\mathbf{c}}_m \\ & \sim \mathcal{CN} \left(\sqrt{\frac{\beta\delta}{\delta+1}} \mathbf{H}_1^H \Phi^H \tilde{\mathbf{c}}_m, \frac{\beta}{\delta+1} \mathbf{H}_1^H \mathbf{H}_1 \right), \forall m \end{aligned} \quad (13)$$

$$\Omega_d^{1/2} \tilde{\mathbf{d}}_m \sim \mathcal{CN}(\mathbf{0}, \Omega_d), \forall m, \quad (14)$$

where the facts $\Phi^H \Phi = \mathbf{I}_N$ and $\Omega_d = \Omega_d^H$ were used.

Next, since the sum of independent Gaussian vector is still Gaussian distributed [12, Theorem 1.2.14], we can obtain the statistics of the m -th column of aggregated channel \mathbf{Q}^H as follows

$$\mathbf{q}_m \sim \mathcal{CN} \left(\sqrt{\frac{\beta\delta}{\delta+1}} \mathbf{H}_1^H \Phi^H \tilde{\mathbf{c}}_m, \frac{\beta}{\delta+1} \mathbf{H}_1^H \mathbf{H}_1 + \Omega_d \right), \quad (15)$$

where \mathbf{q}_m , $1 \leq m \leq M$, are mutual independent. Therefore, $\text{vec}(\mathbf{Q}^H)$ is a complex Gaussian vector with the following mean and covariance matrices

$$\mathbb{E} \{ \text{vec}(\mathbf{Q}^H) \} = \text{vec} \left(\sqrt{\frac{\beta\delta}{\delta+1}} \mathbf{H}_1^H \Phi^H \tilde{\mathbf{H}}_2^H \right), \quad (16)$$

$$\text{Cov} \{ \text{vec}(\mathbf{Q}^H) \} = \mathbf{I}_M \otimes \left(\frac{\beta}{\delta+1} \mathbf{H}_1^H \mathbf{H}_1 + \Omega_d \right), \quad (17)$$

where vec and \otimes denote the vectorization by column stacking and Kronecker product, respectively.

Then, using the distribution of $\text{vec}(\mathbf{Q}^H)$ and following the notations in [11, Page 2], matrix \mathbf{Q} is a complex Gaussian distributed matrix, written as

$$\mathbf{Q} \sim \mathcal{CN} \left(\sqrt{\frac{\beta\delta}{\delta+1}} \tilde{\mathbf{H}}_2 \Phi \mathbf{H}_1, \mathbf{I}_M \otimes \left(\frac{\beta}{\delta+1} \mathbf{H}_1^H \mathbf{H}_1 + \Omega_d \right) \right). \quad (18)$$

Therefore, the product $\mathbf{Q}^H \mathbf{Q}$ has a complex non-central Wishart distribution [12, Definition 10.3.1], as follows

$$\begin{aligned} \mathbf{Q}^H \mathbf{Q} & \sim \mathcal{W}_K \left(M, \frac{\beta}{\delta+1} \mathbf{H}_1^H \mathbf{H}_1 + \Omega_d \right. \\ & \left. , \left(\frac{\beta}{\delta+1} \mathbf{H}_1^H \mathbf{H}_1 + \Omega_d \right)^{-1} \frac{\beta\delta}{\delta+1} \mathbf{H}_1^H \Phi^H \tilde{\mathbf{H}}_2^H \tilde{\mathbf{H}}_2 \Phi \mathbf{H}_1 \right). \end{aligned} \quad (19)$$

Even though the non-central Wishart distribution (19) is accurate, its statistics are very complicated, and based on which we cannot obtain a tractable expression for insightful analysis. To tackle this challenge, as in contributions [13], [14], we next approximate the non-central Wishart distribution

(19) as a central Wishart distribution with the same first-order moment.

To begin with, the first-order moment for the considered non-central Wishart distribution is [14, (45)]

$$\begin{aligned} & \mathbb{E} \{ \mathbf{Q}^H \mathbf{Q} \} \\ & = M \left(\frac{\beta}{\delta+1} \mathbf{H}_1^H \mathbf{H}_1 + \Omega_d \right) + \frac{\beta\delta}{\delta+1} \mathbf{H}_1^H \Phi^H \tilde{\mathbf{H}}_2^H \tilde{\mathbf{H}}_2 \Phi \mathbf{H}_1 \\ & = M \left(\frac{\beta}{\delta+1} \mathbf{H}_1^H \mathbf{H}_1 + \Omega_d \right) + M \frac{\beta\delta}{\delta+1} \mathbf{H}_1^H \Phi^H \mathbf{a}_N \mathbf{a}_N^H \Phi \mathbf{H}_1, \end{aligned} \quad (20)$$

where the last equality is obtained by using (5) and $\mathbf{a}_M^H \mathbf{a}_M = M$.

Therefore, a virtual central Wishart distribution with this moment is given by [14, Sec. V. A]

$$\begin{aligned} & \mathbf{Q}^H \mathbf{Q} \sim \\ & \mathcal{W}_K \left(M, \frac{\beta}{\delta+1} \mathbf{H}_1^H \mathbf{H}_1 + \Omega_d + \frac{\beta\delta}{\delta+1} \mathbf{H}_1^H \Phi^H \mathbf{a}_N \mathbf{a}_N^H \Phi \mathbf{H}_1 \right). \end{aligned} \quad (21)$$

Based on the obtained complex central Wishart distribution (21), with the help of [15, Table I], we can calculate the expectation of the matrix inverse as follows

$$\begin{aligned} & \mathbb{E} \{ (\mathbf{Q}^H \mathbf{Q})^{-1} \} \\ & = \frac{\left(\frac{\beta}{\delta+1} \mathbf{H}_1^H \mathbf{H}_1 + \Omega_d + \frac{\beta\delta}{\delta+1} \mathbf{H}_1^H \Phi^H \mathbf{a}_N \mathbf{a}_N^H \Phi \mathbf{H}_1 \right)^{-1}}{M - K}. \end{aligned} \quad (22)$$

Substituting (22) into (9), we can obtain the ergodic rate of user k , which is shown in (24) at the top of the next page. Note that the derived expression, (24), only depends on the statistical CSI, since the instantaneous CSI-related variables have been averaged out. Therefore, the RIS design based on (24) only needs to be done on a large time-scale, which effectively reduces the overhead. Besides, it is clear that (24) is an increasing function of p and the RIS-BS channel strength β , but it is a decreasing function of noise power σ^2 .

Corollary 1 *The rate in (24) is on the order of $\mathcal{O}(\log_2(M))$. As $M \rightarrow \infty$, the rate can maintain non-zero when the power is scaled down proportionally to $p = 1/M$.*

Proof: It can be proved by noting that all the matrices in the denominator of (24) do not depend on M . ■

Corollary 2 *When $M \rightarrow \infty$ or $p \rightarrow \infty$, RIS-aided massive MIMO systems with ZF detectors perform much better than that with MRC detectors.*

Proof: Based on (24), when $M \rightarrow \infty$ or $p \rightarrow \infty$, we have $R_k \rightarrow \infty$, while the rate in RIS-aided massive MIMO systems with MRC detectors is still bounded due to the multi-user interference, as proved in [10, (7)]. ■

Corollary 3 *When $\beta = 0$, i.e., without the existence of the RIS, the rate of user k reduces to*

$$R_k \geq \log_2 \left(1 + p(M - K) \gamma_k / \sigma^2 \right), \quad (23)$$

which is the same rate as [16, (20)], and its gain is on the order of $\mathcal{O}(\log_2(M))$.

$$R_k \geq \log_2 \left(1 + \frac{p(M-K)}{\sigma^2(\delta+1)} \times \frac{1}{\left[(\mathbf{B}\mathbf{H}_1^H\mathbf{H}_1 + (\delta+1)\mathbf{\Omega}_d + \beta\delta\mathbf{H}_1^H\mathbf{\Phi}^H\mathbf{a}_N\mathbf{a}_N^H\mathbf{\Phi}\mathbf{H}_1)^{-1} \right]_{kk}} \right), 1 \leq k \leq K. \quad (24)$$

Corollary 4 When $\delta = 0$, the rate of user k is

$$R_k \geq \log_2 \left(1 + \frac{p}{\sigma^2} \frac{M-K}{\left[(\mathbf{B}\mathbf{H}_1^H\mathbf{H}_1 + \mathbf{\Omega}_d)^{-1} \right]_{kk}} \right). \quad (25)$$

When $N \rightarrow \infty$, it can be further approximated as

$$R_k \geq \log_2 (1 + p(M-K)(N\alpha_k\beta + \gamma_k)/\sigma^2), \quad (26)$$

which is an increasing function of p , M , N , α_k , β and γ_k , and its gain is on the order of $\mathcal{O}(\log_2(MN))$.

Proof: Note that the k -th diagonal element of $\mathbf{H}_1^H\mathbf{H}_1$ equals $\alpha_k N$, while the non-diagonal elements are not proportional to N . When $N \rightarrow \infty$, we can approximate $\mathbf{H}_1^H\mathbf{H}_1$ as $N\text{diag}\{\alpha_1, \dots, \alpha_K\}$. Then, the proof can be completed. ■

Corollary 4 corresponds to the systems where the propagation environment between the RIS and the BS is rich scattering. This may happen when the RIS is far away from the BS. In this setup, (26) reveals a very promising capacity gain. It is well-known that a gain $\mathcal{O}(\log_2(MN^2))$ is achievable for RIS-aided single-user systems [5]. Here, we prove that by using ZF detectors and in the multi-user setup, a gain $\mathcal{O}(\log_2(MN))$ is still achievable. Besides, under the condition in Corollary 4, it is shown that the RIS-aided massive MIMO systems with ZF detectors always outperform RIS-free massive MIMO systems.

Next, we design the RIS phase shifts based on (24). The sum-rate maximization problem can be formulated as follows

$$\max_{\mathbf{\Phi}} R^s = \sum_{k=1}^K R_k, \quad (27a)$$

$$\text{s.t. } |e^{j\theta_n}| = 1, \quad 1 \leq n \leq N. \quad (27b)$$

Problem (27) can be solved by a gradient ascent method.

Lemma 1 Treat \mathbf{v} as the optimized variable. The gradient vector of the sum rate function $R^s(\mathbf{v})$ is given by

$$\frac{\partial R^s(\mathbf{v})}{\partial \mathbf{v}^*} = \sum_{k=1}^K \frac{\frac{\mathbf{B}\mathbf{v}}{\mathbf{v}^H\mathbf{A}_k\mathbf{v}} - \frac{\mathbf{v}^H\mathbf{B}\mathbf{v}\mathbf{A}_k\mathbf{v}}{(\mathbf{v}^H\mathbf{A}_k\mathbf{v})^2}}{\ln(2) \left(1 + \frac{\mathbf{v}^H\mathbf{B}\mathbf{v}}{\mathbf{v}^H\mathbf{A}_k\mathbf{v}} \right)}, \quad (28)$$

where

$$\mathbf{A}_k = \frac{\sigma^2(\delta+1)}{p(M-K)} \left([\mathbf{\Lambda}^{-1}]_{kk} \mathbf{B} - \beta\delta\mathbf{s}_k\mathbf{s}_k^H \right), \quad (29)$$

$$\mathbf{B} = \frac{1}{N} \mathbf{I}_N + \beta\delta \text{diag}(\mathbf{a}_N^H) \mathbf{H}_1 \mathbf{\Lambda}^{-1} \mathbf{H}_1^H \text{diag}(\mathbf{a}_N), \quad (30)$$

with $\mathbf{\Lambda} = \mathbf{\Lambda}^H \triangleq \beta\mathbf{H}_1^H\mathbf{H}_1 + (\delta+1)\mathbf{\Omega}_d$, and $\mathbf{s}_k^H \triangleq [\mathbf{\Lambda}^{-1}\mathbf{H}_1^H \text{diag}(\mathbf{a}_N)]_{(k,:)}$ corresponds to the k -th row vector.

Proof: By defining $\mathbf{\Lambda}$ and \mathbf{s}_k^H , and using the Woodbury's identity, we can rewrite the k -th diagonal entry in (24) as

$$\begin{aligned} & \left[(\mathbf{\Lambda} + \beta\delta\mathbf{H}_1^H\mathbf{\Phi}^H\mathbf{a}_N\mathbf{a}_N^H\mathbf{\Phi}\mathbf{H}_1)^{-1} \right]_{kk} \\ &= \left[(\mathbf{\Lambda} + \beta\delta\mathbf{H}_1^H \text{diag}(\mathbf{a}_N) \mathbf{v}\mathbf{v}^H \text{diag}(\mathbf{a}_N^H) \mathbf{H}_1)^{-1} \right]_{kk} \\ &= [\mathbf{\Lambda}^{-1}]_{kk} - \frac{\beta\delta [\mathbf{\Lambda}^{-1}\mathbf{H}_1^H \text{diag}(\mathbf{a}_N) \mathbf{v}\mathbf{v}^H \text{diag}(\mathbf{a}_N^H) \mathbf{H}_1 \mathbf{\Lambda}^{-1}]_{kk}}{1 + \beta\delta\mathbf{v}^H \text{diag}(\mathbf{a}_N^H) \mathbf{H}_1 \mathbf{\Lambda}^{-1} \mathbf{H}_1^H \text{diag}(\mathbf{a}_N) \mathbf{v}} \\ &= \frac{\mathbf{v}^H \{ [\mathbf{\Lambda}^{-1}]_{kk} \mathbf{B} - \beta\delta\mathbf{s}_k\mathbf{s}_k^H \} \mathbf{v}}{\mathbf{v}^H \mathbf{B} \mathbf{v}}. \end{aligned} \quad (31)$$

Then, by defining \mathbf{A}_k , using (24) and (31), the sum rate can be rewritten as $R^s = \sum_{k=1}^K \log_2 \left(1 + \frac{\mathbf{v}^H \mathbf{B} \mathbf{v}}{\mathbf{v}^H \mathbf{A}_k \mathbf{v}} \right)$. Based on the chain rule, the gradient of a real function with respect to complex vector variable is given by [17]

$$\frac{\partial R^s(\mathbf{v})}{\partial \mathbf{v}^*} = \sum_{k=1}^K \frac{1}{\ln(2) \left(1 + \frac{\mathbf{v}^H \mathbf{B} \mathbf{v}}{\mathbf{v}^H \mathbf{A}_k \mathbf{v}} \right)} \frac{\partial \left(\frac{\mathbf{v}^H \mathbf{B} \mathbf{v}}{\mathbf{v}^H \mathbf{A}_k \mathbf{v}} \right)}{\partial \mathbf{v}^*}. \quad (32)$$

Using $\frac{\partial \{\mathbf{v}^H \mathbf{B} \mathbf{v}\}}{\partial \mathbf{v}^*} = \mathbf{B} \mathbf{v}$, and $\frac{\partial \{\mathbf{v}^H \mathbf{A}_k \mathbf{v}\}}{\partial \mathbf{v}^*} = \mathbf{A}_k \mathbf{v}$, we have

$$\begin{aligned} \frac{\partial \left(\frac{\mathbf{v}^H \mathbf{B} \mathbf{v}}{\mathbf{v}^H \mathbf{A}_k \mathbf{v}} \right)}{\partial \mathbf{v}^*} &= \frac{\left\{ \frac{\partial (\mathbf{v}^H \mathbf{B} \mathbf{v})}{\partial \mathbf{v}^*} \right\} \mathbf{v}^H \mathbf{A}_k \mathbf{v} - \mathbf{v}^H \mathbf{B} \mathbf{v} \left\{ \frac{\partial (\mathbf{v}^H \mathbf{A}_k \mathbf{v})}{\partial \mathbf{v}^*} \right\}}{(\mathbf{v}^H \mathbf{A}_k \mathbf{v})^2} \\ &= \frac{\mathbf{B} \mathbf{v} \mathbf{v}^H \mathbf{A}_k \mathbf{v} - \mathbf{v}^H \mathbf{B} \mathbf{v} \mathbf{A}_k \mathbf{v}}{(\mathbf{v}^H \mathbf{A}_k \mathbf{v})^2} = \frac{\mathbf{B} \mathbf{v}}{\mathbf{v}^H \mathbf{A}_k \mathbf{v}} - \frac{\mathbf{v}^H \mathbf{B} \mathbf{v} \mathbf{A}_k \mathbf{v}}{(\mathbf{v}^H \mathbf{A}_k \mathbf{v})^2}. \end{aligned} \quad (33)$$

Substituting (33) into (32) completes the proof. ■

Assume the variable in the t -th iteration is \mathbf{v}^t . Then, the variable in the $(t+1)$ -th iteration is updated as

$$\mathbf{v}^{t+1} = \exp \left(j \arg \left(\mathbf{v}^t + \frac{\partial R^s(\mathbf{v})}{\partial \mathbf{v}^*} \bigg|_{\mathbf{v}=\mathbf{v}^t} \right) \right), \quad (34)$$

and the iteration is terminated when the change of sum rate is less than 10^{-4} . Due to the page limit, the detailed pseudocode for the gradient ascent algorithm can be found in [6].

IV. SIMULATION RESULTS

Unless otherwise stated, we consider $K = 4$ users evenly located on the half-circle centered of an RIS with a radius $d_{UI} = 20$ m. The distance between the RIS and the BS is $d_{IB} = 700$ m. Using d_{UI} and d_{IB} , the distance between the users and the BS can be calculated by their geometric relationship as [10]. Based on the distances, the path loss factors α_k , β and γ_k are calculated the same as [10]. Besides, we set $M = N = 64$, $p = 30$ dBm, $\delta = 1$ and $\sigma^2 = -104$ dBm. The angles in the LoS channels are generated randomly from $[0, 2\pi]$.

In Fig. 2, we can observe the obvious superiority of ZF-based RIS design over the random phase shifts-based design,

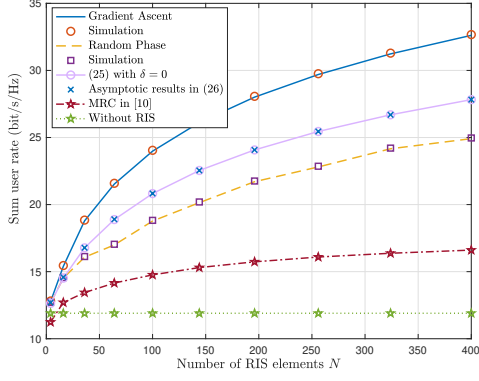


Fig. 2. Rate versus the number of RIS elements N .

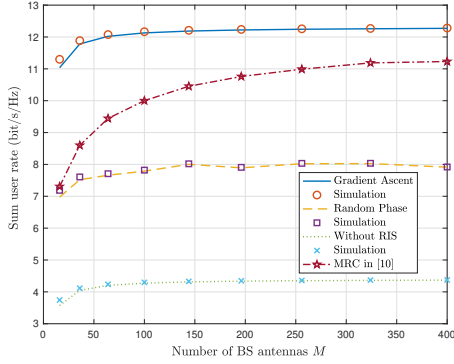


Fig. 3. Rate versus M , where power is scaled down as $p = 10/M$.

the MRC-based design, and the RIS-free systems. When $\delta = 0$, we also validate the accuracy of Corollary 4. In Fig. 3, we verify the power scaling law as expected in Corollary 1. It again emphasizes the advantages of ZF-based RIS systems. Besides, all numerical results show that the derived lower bound is very tight.

Fig. 4 plots the rate versus Rician factor δ . We can find that when $d_{IB} = 700$ m, the rate with large δ performs worse, while a contrary result is observed when $d_{IB} = 300$ m. This is because when d_{IB} is large, the direct channel becomes weak, and then the cascaded channel \mathbf{G} becomes a dominant factor. In this case, when δ is large, the channel \mathbf{G} becomes rank-deficient, which degrades the rate. However, when d_{IB} is small, the direct links are strong. Since the direct links have full-rank, the aggregate channel could always have full-rank. As shown in (24), the variable Φ can play more roles when δ is large, which results in large performance gains. In addition, we can see that it is fair to analyze the rate scaling law in the setup of $\delta = 0$, which validates the universality of conclusions drawn in Corollary 4.

V. CONCLUSION

An RIS-aided massive MIMO system with ZF detectors was considered in this paper. We derive and optimize the ergodic rate, and then reveal that the ergodic rate can achieve a gain of $\mathcal{O}(\log_2(MN))$.

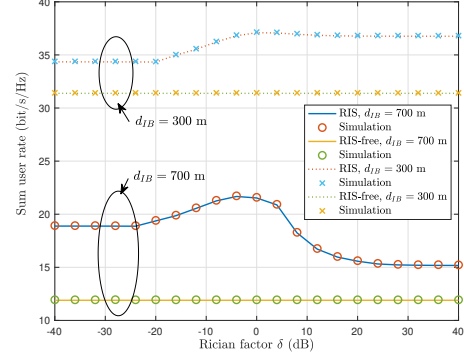


Fig. 4. Rate versus the Rician factor δ .

REFERENCES

- [1] C. Pan, H. Ren, K. Wang, J. F. Kolb *et al.*, "Reconfigurable intelligent surfaces for 6G systems: Principles, applications, and research directions," *IEEE Commun. Mag.*, vol. 59, no. 6, pp. 14–20, Jun. 2021.
- [2] X. Yuan, Y.-J. A. Zhang, Y. Shi, W. Yan, and H. Liu, "Reconfigurable-intelligent-surface empowered wireless communications: Challenges and opportunities," *IEEE Wireless Commun.*, vol. 28, no. 2, pp. 136–143, Apr. 2021.
- [3] C. Pan, H. Ren, K. Wang, M. ElKashlan, A. Nallanathan, J. Wang, and L. Hanzo, "Intelligent reflecting surface aided MIMO broadcasting for simultaneous wireless information and power transfer," *IEEE J. Sel. Areas Commun.*, vol. 38, no. 8, pp. 1719–1734, Aug. 2020.
- [4] C. Pan *et al.*, "Multicell MIMO communications relying on intelligent reflecting surfaces," *IEEE Trans. Wireless Commun.*, vol. 19, no. 8, pp. 5218–5233, Aug. 2020.
- [5] Y. Han, W. Tang, S. Jin, C.-K. Wen, and X. Ma, "Large intelligent surface-assisted wireless communication exploiting statistical CSI," *IEEE Trans. Veh. Technol.*, vol. 68, no. 8, pp. 8238–8242, Aug. 2019.
- [6] Q. U. A. Nadeem, A. Kammoun, A. Chaaban, M. Debbah, and M. S. Alouini, "Asymptotic max-min SINR analysis of reconfigurable intelligent surface assisted MISO systems," *IEEE Trans. Wireless Commun.*, vol. 19, no. 12, pp. 7748–7764, Dec. 2020.
- [7] M. M. Zhao, Q. Wu, M. J. Zhao, and R. Zhang, "Intelligent reflecting surface enhanced wireless networks: Two-timescale beamforming optimization," *IEEE Trans. Wireless Commun.*, vol. 20, no. 1, pp. 2–17, Jan. 2021.
- [8] Y. Jia, C. Ye, and Y. Cui, "Analysis and optimization of an intelligent reflecting surface-assisted system with interference," *IEEE Trans. Wireless Commun.*, vol. 19, no. 12, pp. 8068–8082, Dec. 2020.
- [9] Y. Gao, J. Xu, W. Xu, D. W. K. Ng, and M. S. Alouini, "Distributed IRS with statistical passive beamforming for MISO communications," *IEEE Wireless Commun. Lett.*, vol. 10, no. 2, pp. 221–225, Feb. 2021.
- [10] K. Zhi, C. Pan, H. Ren, and K. Wang, "Statistical CSI-based design for reconfigurable intelligent surface-aided massive MIMO systems with direct links," *IEEE Wireless Commun. Lett.*, vol. 10, no. 5, pp. 1128–1132, May 2021.
- [11] S. Jin, X. Gao, and X. You, "On the ergodic capacity of rank-1 rician-fading MIMO channels," *IEEE Trans. Inf. Theory*, vol. 53, no. 2, pp. 502–517, Feb. 2007.
- [12] R. J. Muirhead, *Aspects of multivariate statistical theory*. John Wiley & Sons, 2009, vol. 197.
- [13] C. Siriteanu, Y. Miyayaga, S. D. Blostein, S. Kuriki, and X. Shi, "MIMO zero-forcing detection analysis for correlated and estimated rician fading," *IEEE Trans. Veh. Tech.*, vol. 61, no. 7, pp. 3087–3099, Sep. 2012.
- [14] C. Siriteanu, A. Takemura, S. Kuriki, D. S. P. Richards, and H. Shin, "Schur complement based analysis of MIMO zero-forcing for rician fading," *IEEE Trans. Wireless Commun.*, vol. 14, no. 4, pp. 1757–1771, Apr. 2015.
- [15] J. A. Tague and C. I. Caldwell, "Expectations of useful complex wishart forms," *Multidimensional Syst. Signal Process.*, vol. 5, no. 3, pp. 263–279, Jul. 1994.
- [16] H. Q. Ngo, E. G. Larsson, and T. L. Marzetta, "Energy and spectral efficiency of very large multiuser MIMO systems," *IEEE Trans. Commun.*, vol. 61, no. 4, pp. 1436–1449, Apr. 2013.
- [17] R. Hunger, "An introduction to complex differentials and complex differentiability," 2007.